The ISME Journal (2009) 3, 266–270

www.nature.com/ismej

SHORT COMMUNICATION

Natural acidophilic biofilm communities reflect distinct organismal and functional organization

Paul Wilmes[1], Jonathan P Remis[2], Mona Hwang[3], Manfred Auer[2], Michael P Thelen[3] and Jillian F Banfield[1,4]

[1]*Department of Earth and Planetary Science, University of California at Berkeley, Berkeley, CA, USA;* [2]*Life Sciences Division, Lawrence Berkeley National Laboratory, Berkeley, CA, USA;* [3]*Chemistry Directorate, Lawrence Livermore National Laboratory, Livermore, CA, USA and* [4]*Department of Environmental Science, Policy and Management, University of California at Berkeley, Berkeley, CA, USA*

Pellicle biofilms colonize the air–solution interface of underground acid mine drainage (AMD) streams and pools within the Richmond Mine (Iron Mountain, Redding, CA, USA). They exhibit relatively low species richness and, consequently, represent good model systems to study natural microbial community structure. Fluorescence *in situ* hybridization combined with epifluorescent microscopy and transmission electron microscopy revealed spatially and temporally defined microbial assemblages. *Leptospirillum* group II dominates the earliest developmental stages of stream pellicles. With increasing biofilm maturity, the proportion of archaea increases in conjunction with the appearance of eukaryotes. In contrast, mature pool pellicles are stratified with a densely packed bottom layer of *Leptospirillum* group II, a less dense top layer composed mainly of archaea and no eukarya. Immunohistochemical detection of *Leptospirillum* group II cytochrome 579 indicates a high abundance of this protein at the interface of the biofilm with the AMD solution. Consequently, community architecture, which most likely develops in response to chemical gradients across the biofilm, is reflected at the functional gene expression level.
The ISME Journal (2009) **3,** 266–270; doi:10.1038/ismej.2008.90; published online 9 October 2008
Subject Category: microbial ecology and functional diversity of natural habitats
Keywords: acid mine drainage; architecture; biofilm; fluorescence *in situ* hybridization; structure and function

Biofilms harboring complex assemblages of microorganisms play essential roles in the Earth's biogeochemical cycles as well as in human disease (Hall-Stoodley *et al.*, 2004). Although they can be readily observed in the natural environment, microscopic studies of their structure and development have mainly focused on single or mixed species cultures grown within laboratory flow cells (O'Toole *et al.*, 2000). Regrettably, *in situ* studies of natural microbial assemblages have been limited (Ramsing *et al.*, 1993; Battin *et al.*, 2003; Domozych and Domozych, 2008; Lemaire *et al.*, 2008).

Biofilms growing within subsurface sulfuric acid solutions (pH ~ 1) and at moderately high temperature (~40 °C) inside the Richmond Mine (Iron Mountain, Redding, CA, USA) exhibit comparatively low species richness (reviewed by Baker and Banfield, 2003) and, hence, represent exquisite model systems for the study of natural microbial assemblages. Comprehensive genomic analyses of acid mine drainage (AMD) biofilms (Tyson *et al.*, 2004; Lo *et al.*, 2007) have facilitated proteomic studies aimed at evaluating microbial activity *in situ* (Ram *et al.*, 2005; Lo *et al.*, 2007). Abundant novel cytochromes central to iron oxidation and, hence, AMD formation have been identified (Cyt_{579} and Cyt_{572}; Ram *et al.*, 2005; Singer *et al.*, 2008; Jeans *et al.*, 2008). However, structural information concerning biofilm development and organization, and possible resulting functional manifestations have so far remained elusive. Such details are essential for our understanding of how microbial communities assemble and function in their natural habitats.

Pellicles floating on top of an underground AMD stream 12 m into the C-drift (C12; Supplementary Figure 1) and those covering a slowly draining underground AMD pool 75 m into the C-drift (C75; Supplementary Figure 1) were sampled on three different occasions spaced over a year period

Correspondence: P Wilmes, Department of Earth and Planetary Science, 307 McCone Hall, University of California at Berkeley, Berkeley, CA 94720, USA.
E-mail: pwilmes@berkeley.edu
Received 12 June 2008; revised 4 August 2008; accepted 4 August 2008; published online 9 October 2008

(6 November 2006, 2 May 2007 and 7 November 2007). C12 is located approximately 63 m downstream from C75 (Supplementary Figure 1). The sampling locations are connected by the flow of AMD solution and, consequently, have similar environmental parameters (Supplementary Table 1). The biofilms sampled in November 2006 likely became detached due to the flooding of the mine with the onset of the winter rains, which typically last from late November and to late March, and grew back when the water levels receded in spring (Edwards *et al.*, 2000; Rudi Carver, *personal communication*). Pellicles were carefully removed from the AMD solutions and their structure preserved (see Supplementary Information for details). Fluorescence *in situ* hybridization (FISH), immunohistochemical detection of Cyt_{579} and microscopy were performed on carefully prepared lateral biofilm sections (see Supplementary Information for details). For each sampling site, date and FISH 16S rRNA probe combination, six biofilm cross-sections were prepared and hybridized. At C12, around 20 mm long transects were prepared from embedded biofilm that covered individual developmental stages (Supplementary Figure 2). The biofilm sections were observed on a standard epifluorescent microscope, a confocal laser scanning microscope (CLSM) and a transmission electron microscope (see Supplementary Information for details). Populations of interest were quantified from CLSM *z*-stacks using the biovolume function in daime (Daims *et al.*, 2006; see Supplementary Information for details). Population numbers were compared using two-way analysis of variance (ANOVA) with replication. From this, the microbial populations at the two sampling sites did not exhibit any statistically significant differences between the three distinct sampling dates ($P>0.5$).

Where the C12 biofilm colonizes the surface of an AMD flow, developmental stages are distinguishable by eye (based on biofilm color density as highlighted in Figure 1a). Biofilms grow out from the stream bank into the flowing AMD stream and representative samples were embedded (Figure 1a). Transects along the biofilm from the newest, thinnest regions to the oldest, thickest regions were examined (highlighted in Figure 1a; Supplementary Figure 2). We noted substantial differences in the occurrence, relative abundance and arrangement of the different community members along the thickness transect (Figure 1b). Although a continuum exists, we can differentiate distinct biofilm development stages on the basis of biofilm thickness, organismal abundance and localization of the different organism types (Figure 1b). These are defined as developmental stages 0 to 2, where 0 corresponds to the youngest biofilm and 2 to the most mature biofilm (Figure 1b).

In developmental stage 0, the pellicles consist almost exclusively of the chemoautotrophic Nitrospira phylum bacterium *Leptospirillum* group II (98% of all cells; Figure 1b). *Leptospirillum* group III cells occur in lower abundance as compared with *Leptospirillum* group II in all developmental stages, but increase in abundance with biofilm maturity (up to 12% of all cells; Figure 1b) and their numbers are statistically significantly different between the different developmental stages (ANOVA, $P<0.02$). *Leptospirillum* group III cells do not form large agglomerations but are present as microcolonies or single cells (Supplementary Figure 3). The patchiness of *Leptospirillum* group III may suggest dispersal for the optimization of resource utilization within the biofilm landscape (Battin *et al.*, 2007), which in turn may be linked to its previously suggested keystone role as the sole nitrogen fixer (Tyson *et al.*, 2004, 2005). With increasing biofilm maturity (development stages 1 and 2; Figure 1b), the proportion of archaea (mainly belonging to the order Thermoplasmatales) and eukarya (mainly fungal filaments) increases and their numbers are statistically significantly different between the different developmental stages (ANOVA, $P<0.004$ and $P<0.0004$, respectively). In their most mature state, C12 biofilms reach a maximum thickness of $\sim 200\,\mu m$ (Figure 1b). Beyond this limit, biofilms exhibit extensive refolding with numerous invaginations that may allow for the efficient diffusion of gases and solutes across the biofilm matrix (Figure 1b).

When assessing the distribution of cells within the biofilm matrix by FISH and CLSM, populations appear as compacted masses of cells that cannot be readily distinguished (Figure 1c). However, the application of transmission electron microscopy to biofilm thin sections enables a more detailed assessment of organism location and association (Figure 1d). *Leptospirillum*-type cells [88% of all cells ($n=2439$)] form dense layers in the middle and towards the top of mature C12 biofilms (Figure 1d). In contrast, archaeal cells are less abundant (11% of all cells), are distributed among the *Leptospirilla* (Figure 1e) and appear to be predominantly localized in the upper half of the biofilms (Figures 1b–d). The archaeal pattern of distribution may be a reflection of reliance on dissolved organic carbon provided mainly by the chemoautotroph *Leptospirillum* group II consistent with chemomixotrophic or chemoorganotrophic lifestyles (Dopson *et al.*, 2004).

The presence of fungi and protists only in the later developmental stages (Figure 1b) may indicate a threshold in the availability of fixed carbon provided by bacteria and archaea. In addition to consuming organic by-products (many of which may be toxic to chemoautotrophs; Frattini *et al.*, 2000) and providing essential metabolites, the eukaryotes most likely shape communities in terms of membership and activity (targeted killing by fungi and grazing by protists), provide fast diffusion pathways along hyphal boundaries and impact carbon cycling within the biofilm. Furthermore, abundant fungal filaments in the

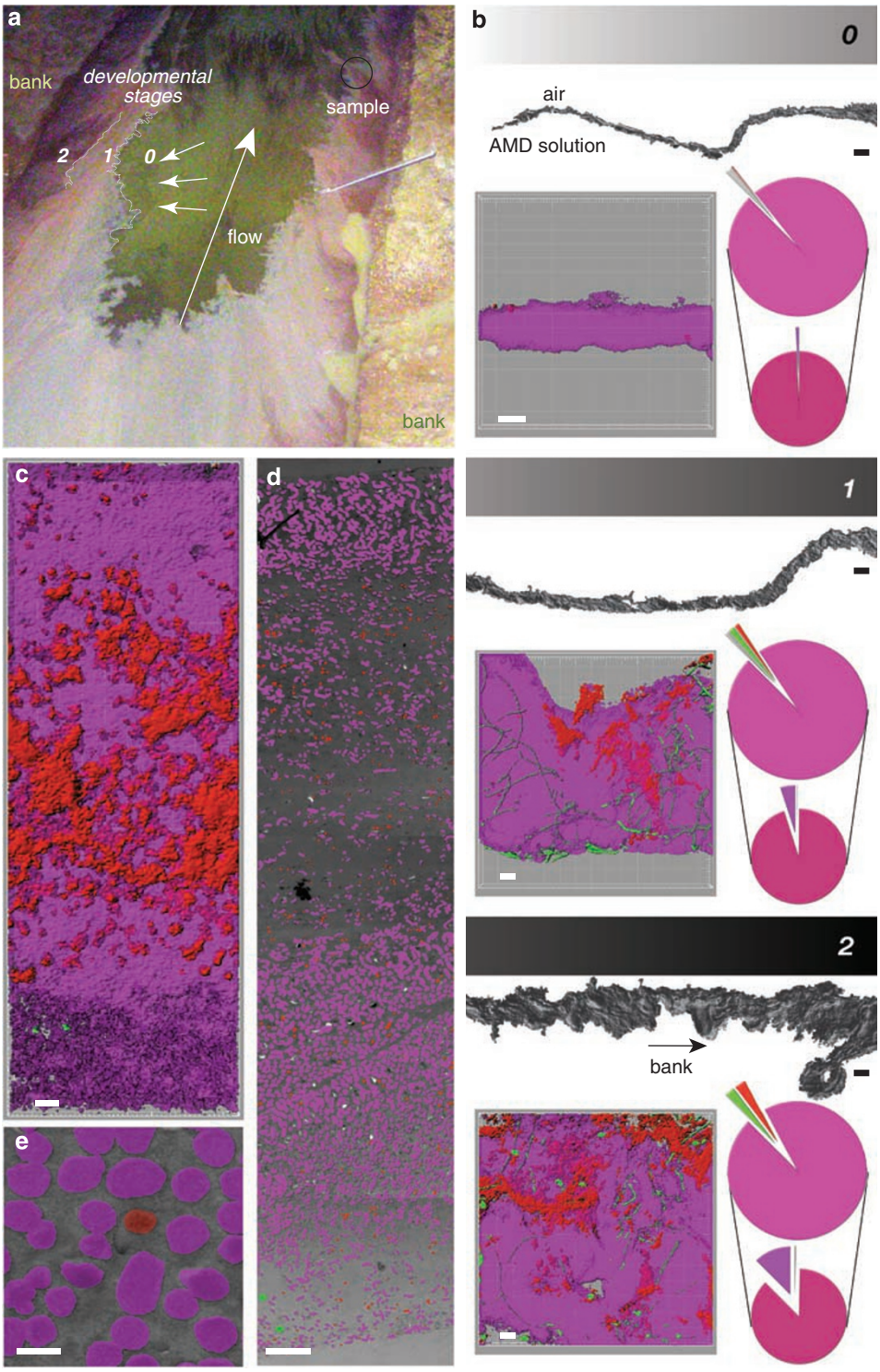

Figure 1 Pellicle biofilm colonizing an acid mine drainage stream. (**a**) Photograph of the C12 sampling location (thermometer placed for scale). Indicated are the direction of flow, the bank, approximate positions of individual development stages and area of sampled biofilm. (**b**) Developmental stages 0–2 from top to bottom: Mosaic of differential interference contrast (DIC) micrographs along the biofilm transect with corresponding three-dimensional confocal laser scanning microscope (CLSM) fluorescence *in situ* hybridization (FISH) micrographs and relative organismal abundances (pie charts). (**c**) Developmental stage 2: three-dimensional CLSM FISH micrograph and (**d**) equivalent transmission electron microscopy (TEM) image montage. (**e**) TEM close-up highlighting differential organismal arrangement. Micrograph and pie chart color-coding: ■ bacteria, ■ archaea, ■ eukarya, ■ *Leptospirillum* group II, ■ *Leptospirillum* group III and ■ unknown. Scale bars are equivalent to 10 μm, except those associated with the mosaics of DIC micrographs in panel c, which are equivalent to 100 μm, and the scale bar in panel e, which is equivalent to 1 μm.

mature C12 biofilms may provide structural support for pellicles subjected to shear stress in flowing streams.

In contrast to the C12 stream biofilms, mature C75 pool biofilms (Figure 2a) are characterized by distinct stratification consisting of a densely packed bottom layer of *Leptospirillum* group II (59% of all cells; Figure 2b) and a less dense top layer comprising mainly archaea (39% of all cells; Figure 2b). Strikingly, eukarya are completely absent from these biofilms. A possible functional manifestation of this bilayer arrangement was assessed by immunohistochemistry using a Cyt_{579}-specific monoclonal antibody (see Supplementary Information for details). This cytochrome plays a central role in iron oxidation by *Leptospirillum* group II and, hence, in AMD generation (Ram *et al.*, 2005; Singer *et al.*, 2008). In contrast to the irregular distribution in the C12 biofilm (Supplementary Figure 4), Cyt_{579} immunofluorescence was primarily localized at the basal side of the C75 biofilm (Figure 2c), suggesting that the majority of iron oxidation catalyzed by Cyt_{579} must occur at the biofilm–solution interface. This observation demonstrates that the distinct organismal arrangement is exquisitely manifest at the functional gene expression level.

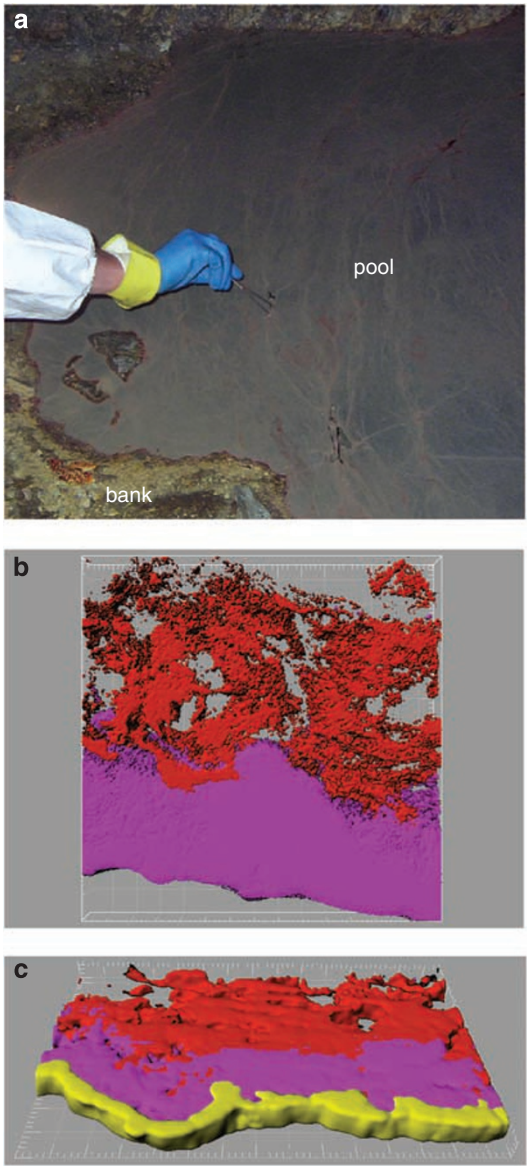

Figure 2 Pellicle biofilm covering an acid mine drainage pool. (**a**) Photograph of the C75 sampling location. (**b**) Confocal laser scanning microscope fluorescence *in situ* hybridization micrograph of cross-sectioned mature biofilm and (**c**) immunohistochemical detection of cytochrome 579 (Cyt_{579}). Micrograph color-coding: ■ *Leptospirillum* group II and III, ■ Archaea, ■ Cyt_{579} monoclonal antibody. Major tick marks in panes (**b** and **c**) are equivalent to 10 μm.

The transition from almost monospecies biofilms to thicker, multispecies, layered communities represents a deterministic process (Battin *et al.*, 2007) and a successional series analogous to those characteristic of macroscopic ecosystems (Connell and Slatyer, 1977). The organismal and functional stratification of the C75 biofilms suggest the existence of micron to tens of micron-scale chemical gradients that span across the biofilm and that currently cannot be measured directly because of the high metal concentrations, low pH and low oxygen solubility in AMD solutions. As the result of fast rates of metabolism relative to diffusion, we anticipate a decline in concentrations of dissolved oxygen, nitrogen, carbon dioxide and in the ferrous to ferric iron ratio with increasing distance from the air–solution interface. The partitioning of *Leptospirillum* group II, the key primary producer in the community, to the lower surface of thicker biofilms at C75 (and the high concentration of Cyt_{579} associated with iron oxidation) suggests that it may be optimized for growth under microaerophilic conditions and this raises the possibility of inter-organism electron transfer. This may take the form of dissolved organic carbon molecules and potential compounds such as hydrogen, nitrogen or sulfur species. The lack of stratification at C12 is attributable to the higher flow rate of the AMD stream (more mixing), which likely increases dissolved gas concentrations and diminishes chemical gradients across the biofilm.

AMD biofilms represent self-contained ecosystems in so far as they are capable of generating all of the biochemical and structural materials necessary for making a living from dissolved ferrous iron, phosphate and trace metals, water and air. The key finding of layering of organisms and function on the micron to tens of micron-scale provides new contextual information for the interpretation of comprehensive genomic and proteomic data available for the constituent organisms (Tyson *et al.*, 2004; Ram *et al.*, 2005; Lo *et al.*, 2007). The combination of ultrastructural information with genomic and proteomic data is a powerful approach for analyzing how microorganisms organize within their environments and contribute to ecosystem function.

Acknowledgements

We thank Mr TW Arman (President, Iron Mountain Mines) and Dr R Sugarek (EPA) for providing site access and Mr D Dodds and Mr R Carver for on site assistance. Linda Kalnejais is acknowledged for the pH and temperature data. We thank Brett Baker, Sheri Simmons, Steve Singer and Vincent Denef for comments and discussions. All current and previous members of the Banfield Lab are acknowledged for sampling at Iron Mountain. We also thank Steve Ruzin and Denise Schichnes for initial help with the confocal microscopy. This work was supported by the United States Department of Energy Genomics:GTL Program (Office of Science).

References

Baker BJ, Banfield JF. (2003). Microbial communities associated with acid mine drainage. *FEMS Microbiol Rev* **44**: 139–152.

Battin TJ, Kaplan LA, Denis Newbold J, Hansen CME. (2003). Contributions of microbial biofilms to ecosystem processes in stream mesocosms. *Nature* **426**: 439–442.

Battin TJ, Sloan WT, Kjelleberg S, Daims H, Head IM, Curtis T *et al.* (2007). Microbial landscapes: new paths to biofilm research. *Nat Rev Microbiol* **5**: 76–81.

Connell JH, Slatyer RO. (1977). Mechanisms of succession in natural communities and their role in community stability and organisation. *Am Nat* **111**: 1119–1144.

Daims H, Lücker S, Wagner M. (2006). Daime, a novel image analysis program for microbial ecology and biofilm research. *Environ Microbiol* **8**: 200–213.

Domozych DS, Domozych CR. (2008). Desmids and biofilms of freshwater wetlands: development and microarchitecture. *Microb Ecol* **55**: 81–93.

Dopson M, Baker-Austin C, Hind A, Bowman JP, Bond PL. (2004). Characterization of *Ferroplasma* isolates and *Ferroplasma acidarmanus* sp. nov., extreme acidophiles from acid mine drainage and industrial bioleaching environments. *Appl Environ Microbiol* **70**: 2079–2088.

Edwards KJ, Bond PL, Druschel GK, McGuire MM, Hamers RJ, Banfield JF. (2000). Geochemical and biological aspects of sulfide mineral dissolution: lessons from Iron Mountain, California. *Chem Geol* **169**: 383–397.

Frattini CJ, Leduc LG, Ferroni GD. (2000). Strain variability and the effects of organic compounds on the growth of the chemolithotrophic bacterium *Thiobacillus ferrooxidans*. *Antonie van Leeuwenhoek* **77**: 57–64.

Hall-Stoodley L, Costerton JW, Stoodley P. (2004). Bacterial biofilms: from the natural environment to infectious diseases. *Nat Rev Microbiol* **2**: 95–108.

Jeans C, Singer SW, Chan CS, VerBerkmoes NC, Shah M, Hettich RL *et al.* (2008). Cytochrome 572 is a conspicuous membrane protein with iron oxidation activity purified directly from a natural acidophilic microbial community. *ISME J* **2**: 542–550.

Lemaire R, Webb RI, Yuan Z. (2008). Micro-scale observations of the structure of aerobic microbial granules used for the treatment of nutrient-rich industrial wastewater. *ISME J* **2**: 528–541.

Lo I, Denef VJ, Verberkmoes NC, Shah MB, Goltsman D, DiBartolo G *et al.* (2007). Strain-resolved community proteomics reveals recombining genomes of acidophilic bacteria. *Nature* **446**: 537–541.

O'Toole G, Kaplan HB, Kolter R. (2000). Biofilm formation as microbial development. *Annu Rev Microbiol* **54**: 49–79.

Ram RJ, VerBerkmoes NC, Thelen MP, Tyson GW, Baker BJ, Blake II RC *et al.* (2005). Community proteomics of a natural microbial biofilm. *Science* **308**: 1915–1920.

Ramsing NB, Kühl M, Jørgensen BB. (1993). Distribution of sulphate-reducing bacteria, O_2, and H_2S in photosynthetic biofilms determined by oligonucleotide probes and microelectrodes. *Appl Environ Microbiol* **59**: 3840–3849.

Singer SW, Chan CS, Zemla A, VerBerkmoes NC, Hwang M, Hettich RL *et al.* (2008). Characterization of cytochrome 579, an unusual cytochrome isolated from an iron oxidizing microbial community. *Appl Environ Microbiol* **74**: 4454–4462.

Tyson GW, Chapman J, Hugenholtz P, Allen EE, Ram RJ, Richardson PM *et al.* (2004). Community structure and metabolism through reconstruction of microbial genomes from the environment. *Nature* **428**: 37–43.

Tyson GW, Lo I, Baker BJ, Allen EE, Hugenholtz P, Baker BJ. (2005). Genome-directed isolation of the key nitrogen fixer *Leptospirillum ferrodiazotrophum* sp nov. from an acidophilic microbial community. *Appl Environ Microbiol* **71**: 6319–6324.

Supplementary Information accompanies the paper on The ISME Journal website (http://www.nature.com/ismej)